

1 **Effect of different carrier gases on productivity**  
2 **enhancement of a novel multi-effect vertical concentric**  
3 **tubular solar brackish water desalination device**

4 Jing Hou<sup>a,b</sup>, Jucai Yang <sup>a</sup>, Zehui Chang <sup>c\*</sup>, Hongfei Zheng <sup>d</sup>, Yuehong Su <sup>e</sup>

5 <sup>a</sup> School of Chemical Engineering College, Inner Mongolia University of Technology, Hohhot ,  
6 010051, China

7 <sup>b</sup> College of mechanical electrical heating and ventilation engine, Inner Mongolia Technical  
8 College of Construction, Hohhot, 010070, China

9 <sup>c</sup> College of Energy and Power Engineering, Inner Mongolia University of Technology, Hohhot,  
10 010051, China

11 <sup>d</sup> School of Mechanical Engineering, Beijing Institute of Technology, Beijing 100081, China

12 <sup>e</sup> Institute of Sustainable Energy Technology, Department of Architecture and Built Environment,  
13 University of Nottingham, Nottingham NG7 2RD, UK

14 \* Corresponding author: E-mail address: changzehui@163.com; Tel.: +86 0471 5278759.

15 **Abstract**

16 A novel multi-effect vertical concentric tubular solar brackish water desalination  
17 device is introduced in present study. The device consists of four closely spaced  
18 concentric pipes, in which the feed water gets preheated by hot brine water to  
19 guarantee the evaporation efficiency. An experimental investigation and analytical  
20 analysis were carried out to signify the effect of carrier gas-water vapor mixture on  
21 productivity enhancement of the device. Different carrier gases were used in the  
22 performance evaluation: carbon dioxide, helium, nitrogen, oxygen, air and argon. The

1 water yield and the top/bottom temperature values of condensation surface of the  
2 device with different carrier gases were tested. In addition, the present investigation is  
3 presented an approach to predict the theory yield based on the internal heat and mass  
4 transfer mechanism. The experimental results indicate that, when the heating  
5 temperature is 80 °C and the carrier gas is helium, the water productivity rate can  
6 reach to 1.19 kg/h. It is increased by 30.76% than the carrier gas of air. The numerical  
7 results had been calculated and a consistent agreement with the experimental results  
8 had been obtained of different operation temperatures. The  $D_v$  under different heating  
9 temperature were obtained according to the experimental results.

10 **Keywords:** Vertical concentric tubular; multi-effect; solar desalination; experimental  
11 comparison; productivity enhancement

## 12 **1. Introduction**

13 Safe and pure drinking water is an important need for life existence and  
14 sustainability. While the earth is covered by approximately 70% water, more than  
15 97.5% of the water is salt and brackish water [1]. Especially, the shortage of fresh  
16 drinking water will appear more obviously for remote or arid regions, but according to  
17 what we know, the existence of great amounts of brackish water in these regions  
18 cannot be ignored. Most of the standard high-capacity desalination methods such as  
19 multi-stage flash, reverse osmosis and multi-effect evaporation, et al are fossil energy  
20 intensive, which lead to global warming as well as health hazards on life. However  
21 these regions are blessed with ample amount of solar energy, so it is attractive  
22 alternative to utilize solar energy for the desalination brackish water to meet potable

1 water need of the residents. Among solar desalination technologies, solar still is used  
2 to produce fresh water from brackish water by utilizing solar energy directly and is  
3 suitable to supply water in these regions for small-scale application due to simple  
4 structure and cost less. However, they have the major drawbacks of lower  
5 productivity compared with conventional solar desalination methods and generally a  
6 single effect [2]. In order to overcome the limitation, many technologies have been  
7 developed to enhance the water production rate and increase the efficiency of solar  
8 still [3-6].

9 Early in 1988 the concept of the tubular solar still (TSS) was proposed by Tiwari  
10 et al. [7]. It is noticed that the area of the condensing surface of tubular solar still is  
11 larger than that of the evaporating surface leading to more yield, which leads to a need  
12 for knowledge of the structure optimization and performance improvement.

13 A novel TSS system was designed by Ahsan et al. [8] to improve the water  
14 production rate of the solar still. The new design has a polythene film cover instead of  
15 the old vinyl chloride sheet. They revealed that the hourly evaporation, condensation  
16 and production rate were affected by the humid air temperature and relative humidity  
17 fraction. In further research, a new mass and transfer model of the TSS was proposed  
18 according to the humid air properties inside the device [9]. Zheng et al. [10] proposed  
19 a novel nonconcentric multi-sleeve horizontal tubular solar still and experimentally  
20 investigated how the water production rate is affected by different carrier gases. The  
21 results indicate that, when the heating temperature is 85 °C, the best carrier gas is  
22 oxygen and the maximum yield can reach to 0.58kg/h. Chang et al. [11] experimental

1 investigated and analytical analyzed a triple-effect vertical concentric solar  
2 desalination device. The Gain Output Ratio (GOR) of the device can reach about 1.89  
3 and the payback period of the unit is about 4.0 year.

4 Xie et al. [12] experimentally and analytically studied the performance of a low  
5 temperature multi-effect tubular solar still (TSS) under different vacuum pressures.  
6 Results show that the peak value of the energy utilization efficiency was 81%. Shitosh  
7 et al. [13] introduced an experimental comparison study on a simple tubular still and  
8 green net covered tubular solar still. Experimental study shows that tubular solar still  
9 covered with green net can increase the yield.

10 Elashmawy et al [14] proposed a tubular solar still integrated with a parabolic  
11 concentrator tracking system (PCST-TSS) and investigated experimentally the  
12 performance compared with other tubular solar stills. According to the results from  
13 the investigation the water production rate of the unit can reach to 1.66L/day. PCST-  
14 TSS costs only \$199 with 45.3% initial cost reduction compared to TSS, which shows  
15 PCST-TSS is suitable to provide water for a single house-hold. An experimental  
16 investigation of a compound parabolic concentrator-concentric tubular solar still  
17 (CPC-CTSS) coupled with a single slope solar still by Arunkumar et al. [15]. It was  
18 found that the yield strongly depends on the evaporative heat transfer coefficient.  
19 They also have tested the performance of CPC-TSS and CPC-CTSS with different  
20 augmentation systems [16].

21 Although a substantial amount of research work has already been carried out to  
22 redesign the structure of TSS and to attempt for enhancement of heat and mass

1 transfer between the evaporation surface and condensation surface. It appears that the  
2 role of thermophysical and transport properties of the different carrier gases and their  
3 effect on the productivity enhancement of the vertical solar desalination device has  
4 been left almost completely unknown. Hence, we propose to improve the yield of the  
5 multi-effect vertical concentric tubular solar brackish water desalination device by  
6 using different carrier gases relative to air is analyzed in detail use a numerical model  
7 of gas-vapor mixture with natural convection to verify. Furthermore, the multi-effect  
8 vertical tubular solar brackish water desalination device presented in this paper can  
9 reuse the latent heat of condensation successfully and guarantee larger effective  
10 evaporation area to gain high energy utilization efficiency.

## 11 **2. The design and operating principle of the device**

### 12 **2.1 Structure parameters and characteristics**

13 Fig.1 illustrates a schematic layout of the multi-effect vertical concentric tubular  
14 brackish water desalination system, Fig. 2 shows a 3D diagram of the system coupled  
15 with vacuum tube solar collector, and Fig. 3 shows a photograph of the experimental  
16 set-up.

**Figure1.** Structure layout of multi-effect vertical concentric tubular solar brackish water desalination system.

1-the brackish water inlet; 2-over flow tube; 3-control valve; 4-the horizontal rubber perforated tube; 5-water film; 6-insulation layer; 7-the 1<sup>st</sup> effect feed water pipe; 8-the 2<sup>nd</sup> effect feed water pipe; 9- the 3<sup>rd</sup> effect feed water pipe; 10- electric heater; 11- hot water tube; 12-outer shell; 13-the water absorption materials; 14-water linerboard; 15-

silicone rubber rings; 16-cold water tube; 17-pressure gages; 18-valve; 19- pressure buffer balloon; 20-brine collection tank; 21-freshwater tank.

**Figure 2.** A 3D diagram of the system coupled with solar collector.

**Figure 3.** A photograph of the experimental set-up.

1           The multi-effect vertical concentric tubular solar brackish water desalination  
2 system is compounded of brackish water tank, vacuum tube solar collector, two water  
3 collection tanks and four circular stainless steel pipes, which form three annulus  
4 sealed spaces that are used as the first-, second-, and third-effect distillation chambers  
5 respectively, while the innermost pipe is filled with hot fresh water as a heat source.  
6 For the convenience of description, three pipes within the corresponding outer shell  
7 may be numbered as 1st, 2nd and 3rd effect from the innermost to the outer. The outer  
8 surface of the 1<sup>st</sup>, 2<sup>nd</sup> and 3<sup>rd</sup> pipes were covered with water absorption materials  
9 (wicking material) knitted with wool, which was adhered tightly by the feed brackish  
10 water and exhausting air between the pipe outer surface and the water absorption  
11 materials. Three horizontal rubber perforated tubes with some holes of 2 mm diameter  
12 which surround across the 1<sup>st</sup>, 2<sup>nd</sup> and 3<sup>rd</sup> pipes round, were placed at the top  
13 bordering edge of the corresponding pipe outside. Brackish water storage tank, which  
14 was placed higher than the pipes and contained a constant water level, supplied the  
15 brackish water via the 1st, 2nd and 3rd effect feed brackish water pipe, which entered  
16 in the corresponding distillation chamber at the bottom of the device and were coiled  
17 on the outside surface of the 1st, 2nd and 3rd effect pipe from bottom to top as shown  
18 in Fig.2, respectively. It is important to emphasize that the feed water was preheated

1 by the hot brackish water film before entering the horizontal rubber perforated tube,  
2 which is beneficial to enhance the fresh water productivity. In order to overcome the  
3 weakness of the non-uniform wetting or dry patches along the water absorption  
4 materials surface, which lead to decrease the effective evaporation area and hence  
5 reducing the distilled yield, several silicone rubber rings were pasted to the water  
6 absorption materials and cotton thread was stitched into the water absorption materials  
7 and form lengthwise horizontal lines and crosswise lines, which means larger  
8 evaporation area than conventional wick.

9 The operational principle of the multi-effect vertical tubular solar brackish water  
10 desalination system is shown in Fig.1 and Fig.2. The water in the hot water container  
11 is heated by the vacuum tube solar collector, by which the brackish water falling film  
12 (5), preheated and drained down the out surface of the 1<sup>st</sup>, 2<sup>nd</sup> and 3<sup>rd</sup> pipes, is heated  
13 up. As the temperature of container water rises, the brackish water in the water  
14 absorption materials (13) will evaporate and the gas in the distillate chamber becomes  
15 saturated with water vapor. The gas-vapor mixture moves towards the relatively cold  
16 inside surface of the outer shell by natural convection due to partial pressure different  
17 between the evaporation and the condensation surface. Meanwhile, the latent heat  
18 released by the vapor is released to heat the brackish water falling film of the 2<sup>nd</sup>  
19 effect. The condensed water then naturally flows downwards to the bottom of the  
20 device and enters in a fresh water collection tank (21) and the un-evaporated brine  
21 leaves the evaporator surface as reject into brine collection tank (20). Similarly, the  
22 evaporation and condensation processes occur in the 2<sup>nd</sup> and 3<sup>rd</sup> distillate chamber and

1 this therefore forms a multi-effect desalination system. The latent heat released by the  
2 water vapor from the 3<sup>rd</sup> effect is eventually dissipated to the environment.

### 3 **3 Prediction of water production of the system filled with different** 4 **carrier gases**

#### 5 3.1 combined heat and mass transfer process in the system

6 Based on the described in the previous section, there are three closed gas-vapor  
7 mixture chambers, which being a vertical annulus space bounded by two stainless  
8 pipes having temperature difference from top to bottom. In order to properly verify  
9 the mass and heat transfer rates for the system mentioned above, it is necessary to  
10 describe the physical phenomena occurring in the device. The heat and mass transfer  
11 processes within the multi-effect vertical solar desalination system are illustrated in  
12 Fig.4.

**Figure. 4** Heat and mass transfer processes in the device.

13 In the first effect, the thin brackish water falling film is heated up by the hot  
14 water container and evaporated from the water absorption materials due to the partial  
15 pressure difference between the 1st effect and the cool inside surface of the 2nd effect.  
16 Then the adjacent carrier gas is heated by the brackish water film mainly by natural  
17 convection and moves up resulting from the density difference due to water vapor  
18 entering into the carrier gas. The carrier gas-water vapor moves from the water  
19 absorption materials to the cool condensation surface by natural convection, which  
20 occurs due to density difference of the carrier gas-water vapor mixture at these two  
21 surfaces, and finally produces the condensation.

1 During the process, the evaporation and condensation of water vapor is affected  
2 by the carrier gas, such as carbon dioxide, helium, nitrogen, oxygen, air and argon.  
3 Some of these gases are lighter and some are heavier than water vapor. This is mainly  
4 because the diffusion and buoyancy force of the vapor for different carrier gas is not  
5 the same. Of simplicity, the carrier-gas-water vapor mixture in the device can be  
6 considered as a whole. Also the carrier gas and water vapor in the device was  
7 assumed to be the ideal gas, respectively.

### 8 3.2 Heat transfer coefficient

9 The heat transfer coefficient in the vertical tubular desalination device depends  
10 on the carrier gas properties, temperature and characteristic size of the convection  
11 chamber, thus it can be expressed as follow:

$$12 \quad h_c = \frac{k}{x_l} \times C \times Ra^n \quad (1)$$

13 where  $x_l$  is the characteristic size of the enclosed space, that is the distance between  
14 the evaporating surface and the condensing surface as to the device proposed above,  
15 m;  $C$  and  $n$  are the numerical constants, which depending on empirical evaluation  
16 from earlier investigation. Reference [17] suggested  $C=0.15$ ,  $n=0.29$  for the vertical  
17 plate enclosed space;  $k$  is working medium thermal conductivity, W/m·K, which  
18 can be calculated using the following empirical correlations developed from  
19 reference [18]:

$$20 \quad k = 0.024 + 0.7673 \times 10^{-4} T_{av} \quad (2)$$

21 For an enclosed space, the natural convection heat transfer process can be  
22 described by the empirical relationship:

1 
$$Ra = Gr \times Pr \quad (3)$$

2 where  $R_a$  is Rayleigh number;  $P_r$  is Prandtl number;  $G_r$  is Grash number.

3 While heat transfer occurs by natural convection, induced by the temperature  
4 difference between two fluid regions is determined for enclosed space by the ordinary  
5 Grash of number [19],

6 
$$Gr = \frac{x_l^3 \times \beta \times g \times \Delta t}{\nu^2} \quad (4)$$

7 where  $\rho$  is the density, kg/m<sup>3</sup>;  $\nu$  is the kinematic viscosity, m<sup>2</sup>/s;  $\beta$  is the volumetric  
8 expansion coefficient, k<sup>-1</sup>;  $\Delta t$  is temperature difference, °C.

9 Inside the device, besides the temperature difference, there exists also a density  
10 difference of the carrier gas-water vapor. When the density of the water vapor is lower  
11 than that of carrier gas, the evaporation naturally increase the buoyancy force thus can  
12 accelerate the heat flow, which leads to the modification of the Grashof number  
13 according to Sharpley and Boelter [20] is:

14 
$$Gr' = \frac{x_l^3 \times g}{\nu_m^2} \left( \frac{\rho_{m,c}}{\rho_{m,e}} - 1 \right) \quad (5)$$

15 Assuming that the working fluid in the device is a binary mixture of the carrier  
16 gas and water vapor in equilibrium, the molecular weights of the mixture at the  
17 evaporation and condensing surface are difference. According to the gas law, the  
18 density of the mixture becomes:

19 
$$\rho_m = \frac{m_a + m_w}{V} = \frac{p_a M_a + p_w M_w}{RT_{av}} = \rho_a + \rho_w \quad (6)$$

20 
$$p_a V = m_a R_{ga} T \quad (7)$$

21 
$$p_w V = m_w R_{gw} T \quad (8)$$

1 where  $R$  is the universal gas constant,  $8.3145\text{J}/(\text{mol}\cdot\text{K})$ ;  $R_g$  is gas constant,  $R_g = R / M$ ;  
 2  $T_{av}$  is the average temperature between the evaporation surface and condensation  
 3 surface;  $p$  is the average pressure. Subscripts:  $a$  is carrier gas;  $w$  is water vapor.

4 The carrier gas-water vapor mixture on the internal surfaces of the unit is in  
 5 saturation, therefore the vapor pressure can be calculated by the following correlation  
 6 derived by fitting of numerical values of saturation vapor pressure between  $10\text{ }^\circ\text{C}$  and  
 7  $110\text{ }^\circ\text{C}$  [20].

$$8 \quad P = 1.131439334 - 3.750393331 \times 10^{-2} \times t + 5.591559189 \times 10^{-3} \times t^2 -$$

$$9 \quad 6.220459433 \times 10^{-5} \times t^3 + 1.10581611 \times 10^{-6} t^4 \quad (9)$$

9 Then the Grash of number modified is calculated by,

$$10 \quad G_r' = \frac{x_l^3 \times \rho^2 \times g}{\mu^2 T_c} \left[ (T_e - T_c) + \frac{(p_e - p_c) \times T_e \times (M_a - M_w)}{M_a P_T - p_{ew} (M_a - M_w)} \right] \quad (10)$$

11 where  $\mu$  is the dynamic viscosity;  $p_T$  is the total pressure of the moist air;  $p_T$   
 12  $=101.3\text{kPa}$ ;  $M_a$  is molar mass of the carrier gas;  $M_w$  is molar mass of the water vapor,  
 13  $M_w = 18\text{g/mol}$ .

14 The Prandtl number ( $Pr$ ) for the binary mixture is defined by the following  
 15 equation:

$$16 \quad Pr = \frac{c_{p,a-w} \mu}{k} \quad (11)$$

17 where  $c_{p,a-w}$  is specific heat at constant pressure of humid air in the device cavity,  
 18  $\text{J}/(\text{kg}\cdot\text{K})$ , which can be calculated using the following empirical correlations  
 19 developed from reference [18]:

$$20 \quad c_{p,a-w} = 0.9992 \times 10^3 + 1.4339 \times 10^{-1} T_{av} + 1.101 \times 10^{-4} T_{av}^2 - 6.7581 \times 10^{-8} T_{av}^3 \quad (12)$$

1 where  $T_{av}$  is average temperature of the evaporating surface and condensation surface,  
 2 K.

### 3 3.3 Mass transfer coefficient

4 The mass transfer coefficient of the unit filled with different carrier gas can be  
 5 given as follows:

$$6 \quad h_m = \frac{h_c \times D_{a-w}}{k \times (L_e)^{n'}} \quad (13)$$

7 Where  $h_c$  is heat transfer coefficient, W/m<sup>2</sup>·K;  $L_e$  is Lewis Number;  $n'$  is the  
 8 numerical constants,  $n'=0.33$  for the enclosed space [21];  $D_{a-w}$  is mass diffusion  
 9 coefficient of water vapor in the air, cm<sup>2</sup>/s. It is estimated by the equation from  
 10 reference [19]:

$$11 \quad D_{a-w} = \frac{0.00143T_{av}^{1.75}}{PM_{aw}^{0.5} \left[ \left( \sum v \right)_a^{1/3} + \left( \sum v \right)_w^{1/3} \right]^2} \quad (13)$$

$$12 \quad M_{aw} = \frac{2}{1/M_a + 1/M_w} \quad (14)$$

13 where  $P$  is the total pressure of gas, bar;  $\sum v$  is the molecular diffusion volume of each  
 14 component in the gas-vapor mixture and its value is respectively given in Table1 [22].

<b>Table 1</b> The $\sum v$ of the simple molecules.
--

15 The other derived parameters of the wet carrier gas can be calculated by the  
 16 following polynomial functions [20]:

$$17 \quad \rho = A_o + A_1 t_{av} + A_2 t_{av}^2 + A_3 t_{av}^3 \quad (16)$$

$$18 \quad \mu_m = B_o + B_1 t_{av} + B_2 t_{av}^2 + B_3 t_{av}^3 + B_4 t_{av}^4 \quad (17)$$

19 where  $t_{av}$  is average temperature of the surface evaporating surface and condensing  
 20 surface, °C . The coefficients in the above polynomial functions are shown in Table 2.

**Table 2** The value of the coefficients in Eq.(16) and (17).

1 Combining the expressions above, the mass transfer coefficient of the device can  
2 be derived that:

$$3 \quad h_m = \frac{h_c}{\rho C_{p,a-w} L_e^{1-n}} \quad (18)$$

4 According to the mass transfer mechanism, the mass flow rate of distillate of the  
5 vertical tubular solar brackish water desalination device can be derived by the  
6 following function:

$$7 \quad m = h_m A_e (\rho_e - \rho_c) \quad (19)$$

8 where  $A_e$  is the area of evaporation surface,  $m^2$ ;  $\rho_e$  and  $\rho_c$  are the densities of the vapor  
9 in evaporation surface and condensation surface, respectively.

#### 10 3.4 Mass diffusion coefficient

11 In this paper, different carrier gases are chosen, namely carbon dioxide, helium,  
12 nitrogen, oxygen, air and argon, to be filled in the device. The values of mass  
13 diffusion coefficient of the water vapor in the different carrier gas were calculated  
14 using Equation (13) and presented in Table 3.

**Table 3** Mass diffusion coefficient of vapor in different carrier gas/ $\times 10^{-7}m^2/s$ .

15 From Table 3, the mass diffusion coefficient shows a similar trend with the  
16 variation of the operation temperature. Helium is achieved the biggest mass diffusion  
17 coefficient in both carrier gases. As Eq. (13) and Eq. (19) shown, the yield of the  
18 device is affected by the density difference and mass diffusion coefficient, which is  
19 directly proportional to the temperature.

## 20 4 Experimental rig and conditions

#### 1 4.1 Experimental method and measurement equipment

2 The experimental investigation was carried out in an air flow and temperature  
3 controlled laboratory in Hohhot, China, where the local pressure was approximately  
4 88 kPa and the altitude was approximately 1081 km. The experimental device shown  
5 in Fig.3, which is consisted of four concentric circular stainless steel pipes (304  
6 grade) having 0.03 m gap between them. The main parameters of the experimental  
7 set-up for operational mode are summarized in Table 4.

<b>Table 4</b> Parameters of the experimental set-up.
---

8 In the experiment, the vacuum pump was used to withdraw the dry air from the  
9 device, then the carrier gas chosen was inflated into three enclosed chambers, and  
10 keep the total pressure of the device same as the ambient pressure, which is achieved  
11 by the pressure buffer balloon. The operation was repeated six times. Different carrier  
12 gases were used in the performance evaluation: carbon dioxide, helium, nitrogen,  
13 oxygen, air and argon. For scenarios with constant heating, one electrical heating rod  
14 was inserted into the hot water container instead of vacuum tube solar collector.

15 The heating temperature was monitored by a thermocouple attached in the hot  
16 water container. The evaporation and condensation temperature of every effect inside  
17 the multi-effect vertical tubular desalination device was recorded as an average  
18 temperature of the measured temperatures from three thermocouples, which were  
19 vertically attached on the outer surface of pipes at 0.45 m interval. The values of  
20 temperature measured were recorded by a multi-channel digital recording device. The  
21 feed brackish water flow rate was measured by liquid turbine flow meter and

1 regulated by a needle valve.

2 All sensors attached on the device and instruments were calibrated before being  
3 used to determine their sensitivity. During the experiment, the water production rate  
4 and the temperature under the constant heating conditions were recorded at 10 min  
5 interval and 1 min interval, respectively. The average yield of four times testing data  
6 was adopted as the value of distillate of the device. The instrumentation, their  
7 accuracy and range is show below in Table 5.

<b>Table 5</b> Technical specifications of instruments used in experimental set-up.
---

## 8 **4.2 Experimental error analysis**

9 During the experiment, the contrived error was avoided by operating carefully  
10 and measuring repeatedly. However, there are experimental measuring errors existed  
11 due to thermocouple chosen, thermocouple points placed on the pipes, leakage of  
12 carrier gas and digital weighing balance, which was utilized for measuring the  
13 distillate. The temperature distribution is changed along the pipe height because of the  
14 heat transfer inside the unit mainly transfer up toward. The different temperature  
15 measuring points attached vertically will take place some errors.

## 16 **5. Results and discussion**

### 17 **5.1 Experimental results and analysis**

18 To investigate the effect of different carrier gases and heating temperature on the  
19 water productivity enhancement of the device, a series of tests were performed in  
20 steady state conditions within the range of temperature between 50 °C to 80 °C with a  
21 temperature step of 5 °C. The top temperature of the operation is normally limited to

1 80 °C due to scaling and fouling problems. The experiment took into account the  
2 temperature of the hot water container as the heating temperature. During each test,  
3 the steady station must be kept more than two hours. The temperature, the water  
4 production rate and other parameters were measured and presented in Fig. 5.

**Figure. 5** The variation of water yield with operation temperature at different carrier gases.

5 It can be observed in Fig.5 that the hourly yield of the device filled with helium  
6 is obviously best among the six carrier gases within the range of temperature between  
7 50 °C to 80 °C, while oxygen gives better water yield. When the operation  
8 temperature is 80 °C, the yield performance of the device with air is worst and the  
9 yield of the device with helium can reach to 1.19 kg/h, which is 30.76% higher than  
10 that of air. It is clear from this result that using helium as the carrier gas in multi-  
11 effect vertical tubular desalination system is optimal.

12 Fig.5 also indicates that, under the condition of different carrier gases, the yield  
13 rate of the device increases obviously with the increase of operation temperature. As  
14 shown in Fig.5, the hourly yield increases slowly under the temperature of 60 °C, and  
15 the hourly yield increases sharply when the heating temperature varies from 65 °C to  
16 80 °C. It is found in this study that lower molecular weight gas such as helium is  
17 preferable for higher heat transfer rates especially under higher operation temperature.  
18 When the operation temperature is 80 °C, using helium as carrier gas, the water yield  
19 per hour of the device is more than 3.53 times that of the device at operation  
20 temperature of 50 °C.

1 As derived before, the water production rate of the device depends on the  
2 evaporation surface area, mass transfer coefficient and the density difference, which  
3 are influenced by different carrier gas. The results can also be obtained from the  
4 experiment, under the different carrier gas-water vapor mixture, the condensation of  
5 the vapor inside the device is difference. This behavior can be explained by analyzing  
6 the temperature distribution along the pipe height. The temperature of the outer shell  
7 in the constant heating temperature experiment is shown in Table 6.

<b>Table 6</b> The measured temperature of the shell under constant heating temperature.
--

8 Table 6 shows that, under the conditions of different carrier gas, the temperature  
9 difference between top shell and bottom shell are different. It is noteworthy that the  
10 temperature of the top shell is higher than that of the bottom shell when the carrier gas  
11 is carbon dioxide, air, nitrogen, oxygen and argon. On the contrary, the temperature of  
12 the bottom shell is higher than that of the top shell when the carrier gas is helium.  
13 Since the different carrier gas in the device has different molar masses, the density of  
14 the carrier gas is different. The water vapor generated from the water absorption  
15 materials can be pushed up to the top shell by the heavier carrier gas such as carbon  
16 dioxide, and contrarily it might be pushed down towards the bottom shell by the  
17 lighter gas like helium. So the vapor more likely condenses on the bottom shell for  
18 carrier gas of helium and this therefore causes a higher bottom shell temperature,  
19 which enlarges the effective condensation area and enhance the water yield. The  
20 situation has opposite trends for carbon dioxide et al. as the carrier gas.

## 21 **5.2 Numerical results and comparison with experimental data**

1 The calculated water yield results of the multi-effect vertical tubular desalination  
2 system with different carrier gas were compared with experimental results  
3 respectively, as shown in Fig. 6.

**Figure. 6** The comparison of the predicted water yield with experimental results.

4 The effect of different carrier gas besides air on the enhancement of the water  
5 yield of such vertical tubular solar desalination device has been left almost completely  
6 unknown. Hence, there are no  $C$  and  $n$  obtained from experimental data for these  
7 carrier gases. Since this is only a comparative investigation to evaluate the effect of  
8 choosing different carrier gas on the enhancement of the water yield of such devices,  
9 it is sufficient to evaluate the mass and heat transfer mechanism of carrier gas-vapor  
10 mixture at constant operation temperature. That is to say, here  $C$  and  $n$  values for  
11 those carrier gases also are the same as that of air. The case of numerical constants in  
12 Eq. (1) are considered, i.e., Case:  $C=0.15$  and  $n=0.29$ .

13 Fig.6 illustrates the comparison of total water yield between the calculated  
14 results and measured data as a function of operation temperature. It is apparent that  
15 the predicted values from the derived formula are in conformity with the trend of the  
16 experimental results. For air as the carrier gas, the deviation between the prediction  
17 value and experimental data is the minimum by about 19.34%. The deviation is the  
18 worst for helium as the carrier gas, with the average deviation of about 46.97% and  
19 the biggest deviation up to 59.17%. As assumed before, the water vapor in the device  
20 is lighter than carrier gas, which leads to the evaporation actually increases the driving  
21 force and application of the modified Grash of number. Choice of  $C$  and  $n$  in Eq. (1)

1 would be another reason for this deviation.

## 2 **5. Conclusions**

3 This paper designed a novel multi-effect solar brackish water desalination system  
4 with vertical annulus space, which decreases the heat and mass transfer resistance and  
5 heat loss thus can improve the yield performance. Furthermore, this kind of device has  
6 good characteristics of good bearing pressure and the feed brackish water is preheated  
7 by the hot brine, which has a beneficial effect in enhancing the distillate production.  
8 Experimental and analytical study has been performed on the effect of different  
9 carrier gas on the enhancement of the water yield of the device. It is clear from this  
10 study that using air as a carrier gas in multi-effect vertical tubular desalination system  
11 is not best. The results indicate that the lighter carrier gas such as helium could  
12 enhance the water production. When the carrier gas is helium, the hourly yield of the  
13 device can reach to 1.19 kg at the operation temperature of 80 °C. Under the same  
14 operation temperature, the yield of the device with helium increases about 30.76%,  
15 25.24%, 20.89%, 20.28% and 18.13% contrasting with that of the device with air,  
16 carbon dioxide, argon, nitrogen and oxygen, respectively. The water yield may be  
17 improved through using proper carrier gas. Among the six carrier gases studied,  
18 helium is found to be the best carrier gas to achieve more desalinated water under the  
19 same heating temperature.

20 It was shown that the numerical calculation is able to predict the fresh water  
21 productivity rate of this system. It is interesting to note that the lower molecular like  
22 helium can achieve higher mass diffusion coefficient of water vapor. The comparison

1 between the numerical and experimental results shows a conformity trend of water  
2 yield. The deviation between the prediction value and experimental data for air as  
3 carrier gas is the minimum by about 19.34%.

#### 4 **Appendix**

5 The operation temperature of multi-effect vertical concentric tubular solar  
6 brackish water desalination device is 50 °C and the carrier gas is nitrogen, the  
7 condensation temperature of the 1<sup>st</sup> effect is 41.17 °C, the condensation temperature of  
8 the 2<sup>nd</sup> effect is 37.36 °C and the out shell temperature is 31.99 °C. The average  
9 temperature between the evaporation surface and the condensation surface of the 1<sup>st</sup>,  
10 2<sup>nd</sup> and 3<sup>rd</sup> effect is 45.58 °C, 39.27 °C and 34.68 °C, respectively.

11 The density and dynamic viscosity of the gas-water vapor mixture of the 1<sup>st</sup>, 2<sup>nd</sup>  
12 and 3<sup>rd</sup> effect using Eq. (16) and (17) become

$$13 \quad \rho_1 = 1.0675 \text{ kg} / \text{m}^3 \quad \mu_{m1} = 1.8368 \times 10^{-5} \text{ N} \cdot \text{s} / \text{m}^2$$

$$14 \quad \rho_2 = 1.1002 \text{ kg} / \text{m}^3 \quad \mu_{m2} = 1.8389 \times 10^{-5} \text{ N} \cdot \text{s} / \text{m}^2$$

$$15 \quad \rho_3 = 1.1229 \text{ kg} / \text{m}^3 \quad \mu_{m3} = 1.8357 \times 10^{-5} \text{ N} \cdot \text{s} / \text{m}^2$$

16 The vapor pressure  $p$  of the 1<sup>st</sup>, 2<sup>nd</sup> and 3<sup>rd</sup> effect can be calculated from Eq. (9)

17 as

$$18 \quad p_{e1} = 1.2371 \times 10^4 p_a \quad p_{c1} = 0.7901 \times 10^4 p_a$$

$$19 \quad p_{e2} = 0.7901 \times 10^4 p_a \quad p_{c2} = 0.6445 \times 10^4 p_a$$

$$20 \quad p_{e3} = 0.6445 \times 10^4 p_a \quad p_{c3} = 0.4776 \times 10^4 p_a$$

21 From Eq. (10), the Grash of number modified can be calculated as

$$22 \quad G'_{r1} = 40231.7083 \quad G'_{r2} = 16680.2185 \quad G'_{r3} = 23488.8070$$

1 Specific heat  $c_{p,a-w}$  and working medium thermal conductivity  $k$  at constant  
2 pressure of carrier gas-water vapor mixture in the evaporation-condensation chamber  
3 of the 1<sup>st</sup>, 2<sup>nd</sup> and 3<sup>rd</sup> effect can be calculated from Eq. (2) and (12) as

$$4 \quad k_1 = 0.04886W / m \cdot K \quad c_{p,a-w_1} = 1053.9J/kg \cdot K$$

$$5 \quad k_2 = 0.04837W / m \cdot K \quad c_{p,a-w_2} = 1052.68J/kg \cdot K$$

$$6 \quad k_3 = 0.04802W / m \cdot K \quad c_{p,a-w_3} = 1051.8J/kg \cdot K$$

7 From Eq. (9), the Prandtl number for the binary mixture can be calculated as

$$8 \quad Pr_1 = 0.3963 \quad Pr_2 = 0.4002 \quad Pr_3 = 0.4021$$

9 The heat transfer coefficient of the 1<sup>st</sup>, 2<sup>nd</sup> and 3<sup>rd</sup> effect from Eq. (1) as

$$10 \quad h_{c_1} = 4.0423W / m^2 \cdot K \quad h_{c_2} = 3.1093W / m^2 \cdot K \quad h_{c_3} = 3.4134W / m^2 \cdot K$$

11 The Lewis Number of the 1<sup>st</sup>, 2<sup>nd</sup> and 3<sup>rd</sup> effect for the binary mixture can be  
12 calculated as

$$13 \quad Le_1 = 0.7993 \quad Le_2 = 0.8072 \quad Le_3 = 0.8111$$

14 The total water yield of the multi-effect vertical tubular solar brackish water  
15 desalination device can be calculated using Eq. (19) become

$$16 \quad m = 0.258kg / h$$

## 17 Acknowledgements

18 We gratefully acknowledge the financial support for this research provided by  
19 the National Natural Science Foundation of China (No. 51666013) Projects and  
20 Natural Science Foundation of Inner Mongolia Autonomous Region, China (No.  
21 2013MS0704, 2015MS0545) Projects.

## 1 **Nomenclature**

2  $C$ - constant number

3  $c_p$ - specific heat, J/(kg·K)

4  $D_{a-w}$ - mass diffusion coefficient, m<sup>2</sup>/s

5  $Gr$ - Grash of number

6  $g$ - gravitational constant

7  $h_m$ - mass transfer coefficient, m/s

8  $h_c$ - heat transfer coefficient, W/m<sup>2</sup>·K

9  $k$ - working medium thermal conductivity, W/m·K

10  $Le$ - Lewis Number

11  $M$ - molar mass, kg/mol

12  $n$ - constant number

13  $Pr$ - Prandtl number

14  $p_w$ - vapor pressure, Pa

15  $p_T$ - total vapor pressure, Pa

16  $R$ - universal gas constant, 8.3145J/(mol·K)

17  $Rg$ - gas constant, J/(kg·K)

18  $Ra$ - Rayleigh number

19  $T_{av}$ - average temperature, K

20  $\Delta t$ - temperature difference, °C

21  $t_w$  - condensation temperature, °C.

22  $x_l$ - feature size, m

1  $\beta$ - volumetric expansion coefficient,  $\text{k}^{-1}$

2  $\rho$ - density,  $\text{kg/m}^3$

3  $\mu$ - dynamic viscosity,  $\text{N}\cdot\text{s/m}^2$

4  $\nu$ - kinematic viscosity,  $\text{m}^2/\text{s}$

5  $\Sigma_v$ - molecular diffusion volume

6 Subscripts

7  $a$ - air

8  $e$ - evaporating surface

9  $c$ - condensing surface

10  $m$ - mixed gas

11  $w$ - water vapor

## 12 **References**

13 [1] M Chandrashekar, Yadav Avadhesh. Water desalination system using solar heat:

14 A review, *Renew Sustain Energy Rev* 67 (2017) 1308-1330.

15 [2] P. Durkaieswaran, K. Kalidasa Murugavel. Various special design of single basin

16 passive solar still - a review, *Renew Sustain Energy Rev* 49 (2015) 1048-1060.

17 [3] S.W. Sharshir, M.O.A. El-Samadony, G. L. Peng, et al, Performance enhancement

18 of wick solar still using rejected water from humidification-dehumidification unit

19 and film cooling, *Applied Thermal Engineering* 108 (2016) 1268-1278.

20 [4] S.W. Sharshir, N. Yang, G.L. Peng, et al, Factors affecting solar stills productivity

21 and improvement techniques - A detailed review, *Applied Thermal Engineering*

22 100 (2016) 267-284.

- 1 [5] Zakaria Haddad, Abla Chaker, Ahmed Rahmani, Improving the basin type solar  
2 still performances using a vertical rotating wick, *Desalination* 418 (2017) 71-78.
- 3 [6] Mehrzad Feilizadeh, M.R. Karimi Estahbanati, Amimul Ahsan, et al, Effects of  
4 water and basin depths in single basin solar stills\_ An experimental and theoretical  
5 study, *Renew Sustain Energy Rev* 122 (2016) 174-181.
- 6 [7] G.N. Tiwari, Nocturnal water production by tubular solar stills using waste heat to  
7 preheat brine, *Desalination* 69 (1988) 309-318.
- 8 [8] Amimul Ahsan, Kh. M. Shafiul Islam, Teruyuki Fukuhara, Abdul Halim Ghazali,  
9 Experimental study on evaporation, condensation and production of a new  
10 Tubular Solar Still, *Desalination* 260 (2010) 172-179.
- 11 [9] Amimul Ahsan, Teruyuki Fukuhara, Mass and heat transfer model of Tubular  
12 Solar Still, *Sol. Energy* 84 (2010) 1147-1156.
- 13 [10] H.F. Zheng, Z.H. Chang, Z.H. Zheng, et al, Performance analysis and  
14 experimental verification of a multi-sleeve tubular still filled with different gas  
15 media, *Desalination* 331 (2013) 56-61.
- 16 [11] Z.H. Chang, Y.J. Zheng, Z.Y. Chen, et al, Performance analysis and  
17 experimental comparison of three operational modes of a triple-effect vertical  
18 concentric tubular solar desalination device, *Desalination* 375 (2015) 10-20.
- 19 [12] G. Xie, L.C. Sun, Z.Y. Mu, et al, Conceptual design and experimental  
20 investigation involving a modular desalination system composed of arrayed  
21 tubular solar stills, *Appl Energy* 179 (2016) 972-984.
- 22 [13] Dillu Shitosh, Medhavi Amit, K D Chinchkhede, Performance and economic

- 1 study of desalination in tubular solar still, *Int. J. Engg. Res. & Sci. & Tech.* 4  
2 (2015) 69-78.
- 3 [14] Mohamed Elashmawy, An experimental investigation of a parabolic concentrator  
4 solar tracking system integrated with a tubular solar still, *Desalination* 411 (2017)  
5 1-8.
- 6 [15] T. Arunkumar, R. Velraj, D. Denkenberger, et al. Effect of heat removal on  
7 tubular solar desalting system, *Desalination* 379 (2016) 24-33.
- 8 [16] T. Arunkumar, R. Velraj, D.C. Denkenberger, et al, Productivity enhancements  
9 of compound parabolic concentrator tubular solar stills, *Renew. Energy* 88 (2016)  
10 391-400.
- 11 [17] A. Baïri, Nusselt-Rayleigh correlations for design of industrial elements:  
12 Experimental and numerical investigation of natural convection in tilted square air  
13 filled enclosures, *Energy Convers Manage* 49 (2008) 771-782.
- 14 [18] S. Toyama, T. Aragaki, H. M. Salah, et al, Simulation of a multi-effect solar still  
15 and the static characteristics, *J Chem Eng Japan* 20(1987) 473-478.
- 16 [19] Mousa K. Abu Arabi, Kandi Venkat Reddy, Performance evaluation of  
17 desalination processes based on the humidification dehumidification cycle with  
18 different carrier gases, *Desalination* 156 (2003) 281-293.
- 19 [20] P. T. Tsilingiris, The influence of binary mixture thermophysical properties in the  
20 analysis of heat and mass transfer processes in solar distillation systems, *Sol.*  
21 *Energy* 81 (2007) 1482-1491.
- 22 [21] F.P. Incropera, D.P. DeWitt, T.L. Bergman, et al, *Fundamentals of Heat and*

1 Mass Transfer (Sixth Edition), 2007 231-235.

2 [22] Bruce E. Poling, John M. Prausnitz, John P. O'Connell, The Properties of Gases

3 and Liquids, 2000 633-634.

4

5

6

7

8

9

10

11

12

13

14

15

16

17

18

19

20

21

22

1  
2  
3  
4  
5  
6  
7  
8  
9  
10  
11  
12  
13  
14  
15  
16  
17  
18  
19  
20  
21  
22  
23  
24

### Captions

**Figure 1.** Structure layout of multi-effect vertical concentric tubular solar brackish water desalination system.

1-the brackish water inlet; 2-over flow tube; 3-control valve; 4-the horizontal rubber perforated tube; 5-water film; 6-insulation layer; 7-the 1<sup>st</sup> effect feed water pipe; 8-the 2<sup>nd</sup> effect feed water pipe; 9- the 3<sup>rd</sup> effect feed water pipe; 10- electric heater; 11- hot water tube; 12-outer shell; 13-the water absorption materials; 14-water linerboard; 15- silicone rubber rings; 16-cold water tube; 17-pressure gages; 18-valve; 19- pressure buffer balloon; 20-brine collection tank; 21-freshwater tank.

**Figure 2.** A 3D diagram of the system coupled with solar collector.

**Figure 3.** A photograph of the experimental set-up.

**Figure 4.** Heat and mass transfer processes in the device.

**Figure 5.** The variation of water yield with operation temperature at different carrier gases.

**Figure 6.** The comparison of the predicted water yield with experimental results.

1

2

3

### Figures

4 Figure 1.

5

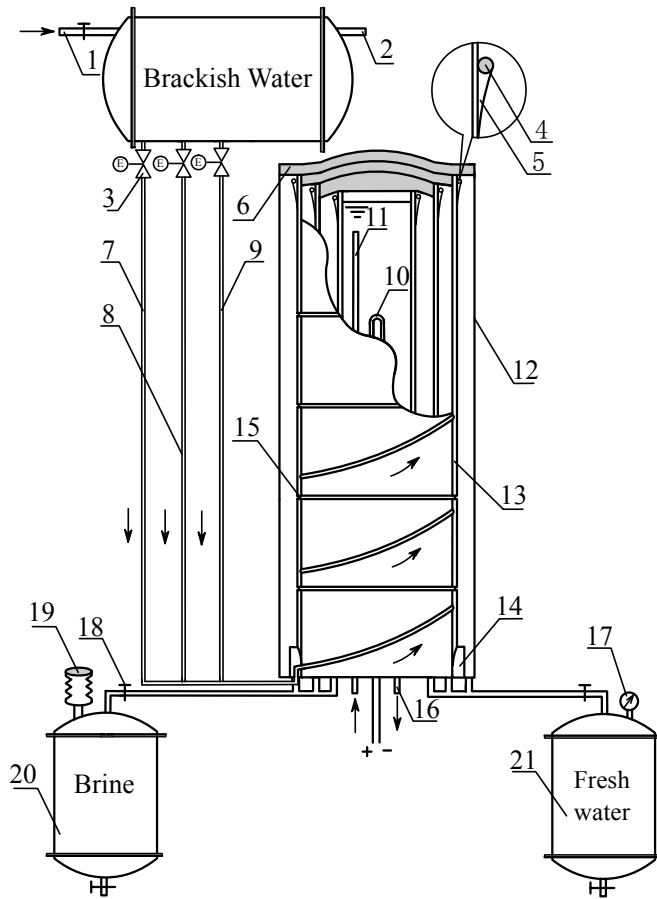
6

7

8

9

10



11

12

13

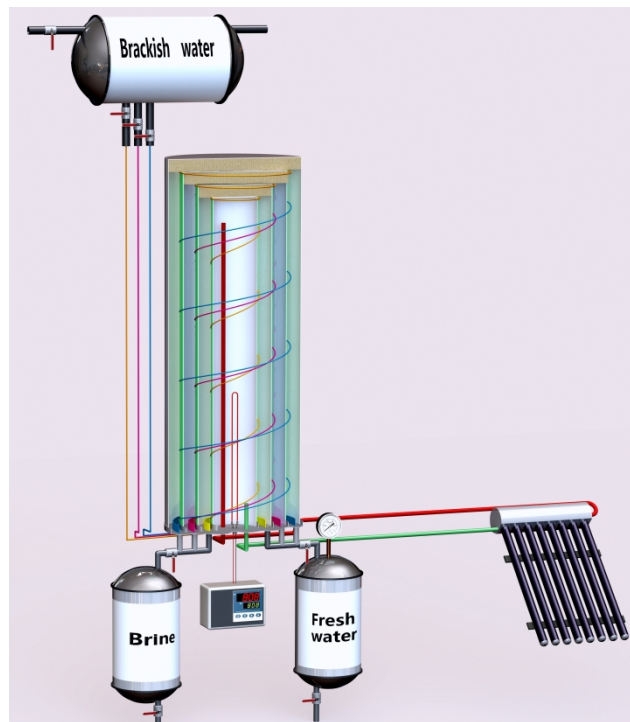
14

15

16

1  
2  
3  
4  
5  
6  
7  
8  
9

Figure 2.



10  
11  
12  
13  
14  
15  
16  
17  
18  
19

1  
2  
3  
4  
5  
6  
7  
8

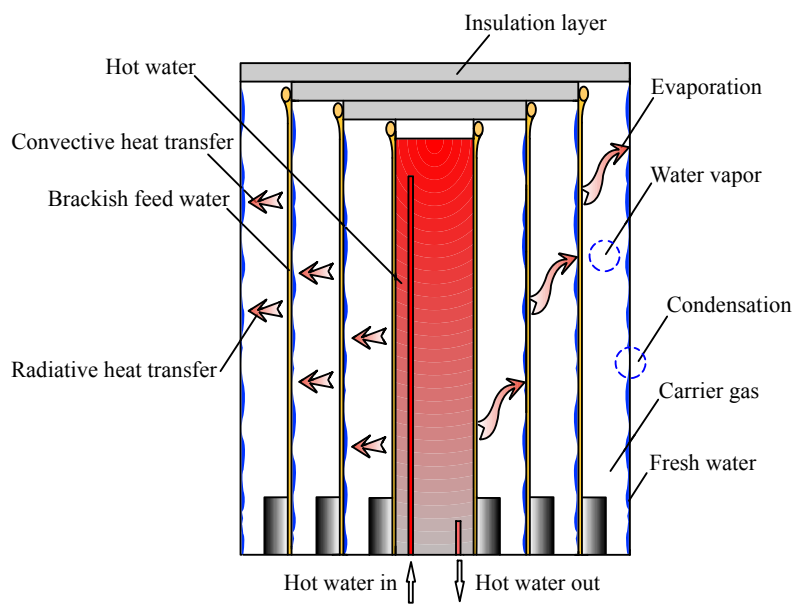
Figure 3.



9  
10  
11  
12  
13  
14  
15  
16  
17  
18  
19  
20  
21

1  
2  
3  
4  
5  
6  
7  
8

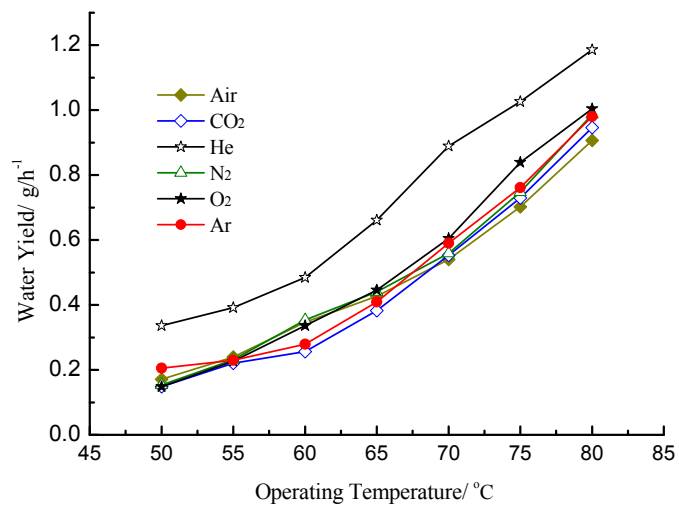
Figure 4.



9  
10  
11  
12  
13  
14  
15  
16  
17  
18  
19  
20

1  
2  
3  
4  
5  
6  
7  
8

Figure 5.

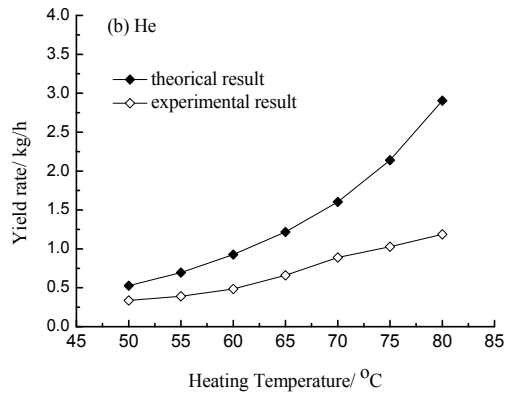
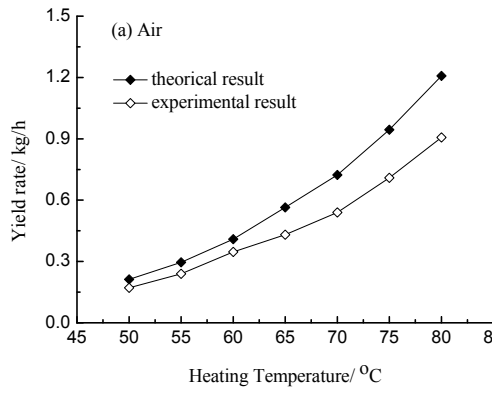


9  
10  
11  
12  
13  
14  
15  
16  
17  
18  
19  
20  
21

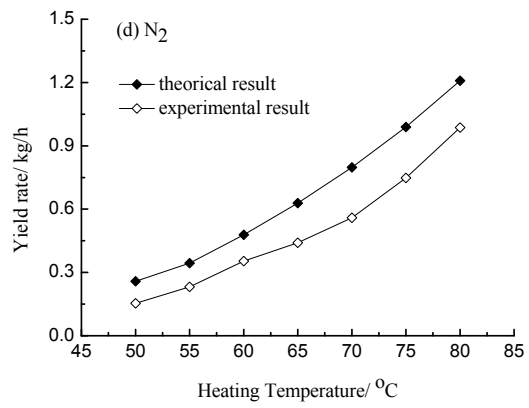
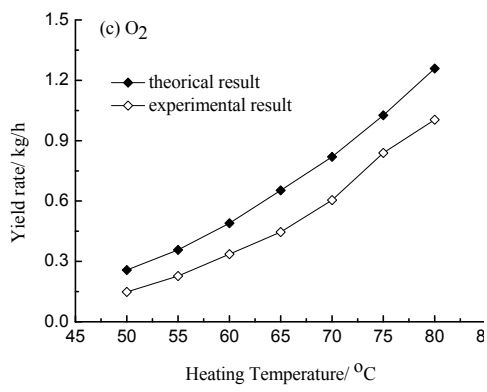
1

2

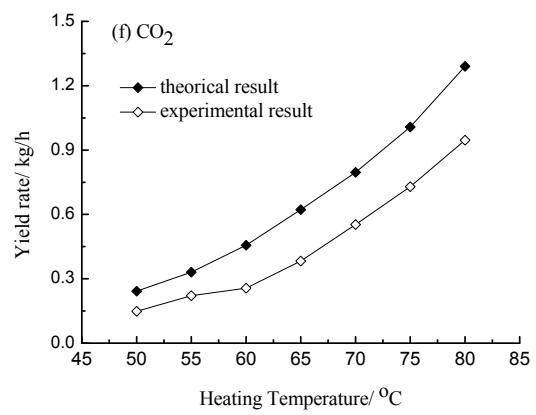
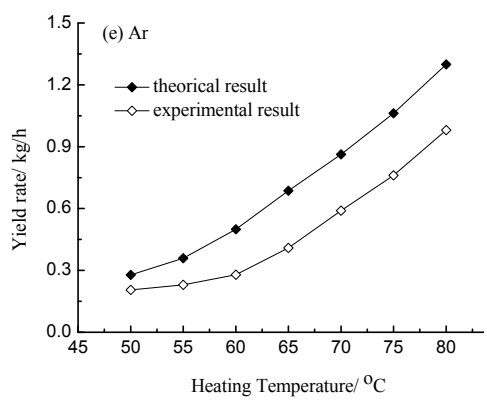
3 Figure 6.



5



7



9

10

1  
2  
3  
4  
5  
6  
7  
8  
9  
10  
11  
12  
13  
14  
15  
16  
17  
18  
19  
20  
21  
22  
23  
24  
25  
26  
27

## Table

**Table 1 The  $\sum v$  of the simple molecules.**

Air	CO <sub>2</sub>	He	N <sub>2</sub>	O <sub>2</sub>	Ar	H <sub>2</sub> O
19.7	26.9	2.67	18.5	16.3	16.2	13.1

1  
2  
3  
4  
5  
6  
7  
8  
9  
10  
11  
12  
13  
14  
15  
16  
17  
18  
19  
20  
21  
22  
23  
24  
25

**Table 2 The value of the coefficients in Eq.(16) and (17).**

( $\text{kg}\cdot\text{m}^{-3}$ )	( $\text{N}\cdot\text{s}\cdot\text{m}^{-2}$ )
$A_0=1.299995662$	$B_0=1.685731754\times 10^{-5}$
$A_1=-6.043625845\times 10^{-3}$	$B_1=9.151853945\times 10^{-8}$
$A_2=4.697926602\times 10^{-5}$	$B_2=-2.16276222\times 10^{-9}$
$A_3=-5.760867827\times 10^{-7}$	$B_3=3.1413922553\times 10^{-11}$
	$B_4=-2.644372665\times 10^{-13}$

1

2 **Table 3 Mass diffusion coefficient of vapor in different carrier gas/ $\times 10^{-7} \text{m}^2/\text{s}$ .**

temperature/ $^{\circ}\text{C}$	Air	He	O <sub>2</sub>	N <sub>2</sub>	CO <sub>2</sub>	Ar
50	290.38	962.54	300.17	295.04	238.62	289.55
60	306.29	1018.44	315.81	310.38	251.32	305.09
70	321.80	1072.37	333.01	327.34	264.76	321.58
80	340.52	1121.74	352.12	345.25	279.57	340.29

3

4

5

6

7

8

9

10

11

12

13

14

15

16

17

18

19

20

21

22

23

24

25

26

1  
2  
3  
4  
5  
6  
7  
8  
9  
10  
11  
12  
13  
14  
15  
16  
17  
18  
19  
20  
21

**Table 4 Parameters of the multi-effect vertical tubular desalination device.**

Number of effects	Heating water tank		The 1 <sup>st</sup> pipe		The 2 <sup>nd</sup> pipe		The 3 <sup>rd</sup> pipe	
	diameter	length	diameter	length	diameter	length	diameter	length
3	100mm	970mm	160mm	980mm	220mm	990mm	280mm	1000mm

1

2 **Table 5 Technical specifications of instruments used in experimental set-up**

---

Instrumentation	Range	Accuracy
Liquid turbine flow meter / Model-109	0.4-4.0 L/h	± 0.1 %
Vacuum pump / V-i180SV	14.4 m <sup>3</sup> /h	± 1.0%
Digital weighing balance / HC ES-02	0.01-500 g	± 0.1%
Multi-channel digital data-recording / TYD-WD	0-300 °C	± 0.5 %
Temperature sensor / K	-120-300 °C	± 0.5 °C

---

3

4

5

6

7

8

9

10

11

12

13

14

15

16

17

18

19

20

21

22

23

1

2 **Table 6 The measured temperature of the shell under constant heating**  
3 **temperature.**

Operation Temperature/°C	Air/°C		CO <sub>2</sub> /°C		He/°C		N <sub>2</sub> /°C		O <sub>2</sub> /°C		Ar/°C	
	Up	Down	Up	Down	Up	Down	Up	Down	Up	Down	Up	Down
50	36.70	31.77	33.05	27.61	32.07	33.37	33.79	28.31	34.35	28.43	33.04	26.85
60	44.82	36.84	41.47	32.56	40.46	44.05	42.37	33.24	41.56	33.63	42.00	32.93
70	52.46	43.35	51.61	39.81	48.01	53.91	53.01	40.72	52.52	41.31	53.24	40.31
80	65.05	54.84	63.69	50.97	56.77	63.70	64.54	52.35	64.75	53.00	65.68	53.13

4